Proceedings Paper:
Yildizbakan, L, Iqbal, N orcid.org/0000-0002-2801-707X, Abdulaziz, D et al. (5 more authors) (2022) Fabrication and Characterisation of Two-Layered Synthetic Titanium-Chitosan Bone Scaffolds. In: TMS 2022 151st Annual Meeting & Exhibition Supplemental Proceedings. TMS 2022 151st Annual Meeting & Exhibition, 27 Feb - 03 Mar 2022, Anaheim, California, USA. Springer, Cham , pp. 768-775. ISBN 9783030923808

https://doi.org/10.1007/978-3-030-92381-5_73

Fabrication and Characterisation of Two-layered Synthetic Titanium-Chitosan Bone Scaffolds

L. Yildizbakan[1], N. Iqbal[1], D. Abdulaziz [1], V. Panagiotopoulou[2], E. Jones[3], N. T. Do[4], P. V. Giannoudis[5], A. Jha[1]

[1]School of Chemical and Process Engineering, University of Leeds, Leeds LS2 9JT, UK

[2] Department of Mechanical Engineering and Aeronautics, University of Patras, Rio 26504, Greece

[3] Clinical Sciences Building, St James University Hospital, School of Medicine, University of Leeds, Leeds LS9 7LN, UK

[4] Division of Oral Biology, St James University Hospital, School of Medicine, University of Leeds, Leeds LS9 7LN, UK

[5]Academic Department of Trauma and Orthopaedic, School of Medicine, University of Leeds, Leeds General Infirmary, Leeds, UK

Email: pmlyi@leeds.ac.uk

ABSTRACT

We have developed two-layered osteoconductive and antibacterial scaffolds, which mimic the natural structure of bone. The synthetic cortical (Type-1) biomaterials were fabricated from porous titanium embedded with 10% iron-doped brushite minerals. The trabecular (Type-2) biomaterials were fabricated from freeze-dried porous chitosan embedded with 10% iron-doped brushite and cerium oxide solution. The Type-1 and Type-2 biomaterials were conjoined during a freeze-drying process in a chamber maintained at -100 ℃ and 40 mTorr pressure; this approach aided the integration of the trabecular and cortical biomaterials, thus forming dual-layered scaffold. The two-layered scaffolds were characterised using Raman, and Fourier Transform Infrared (FTIR) Spectroscopy, Energy-dispersive X-ray (EDX) Spectroscopy and Scanning Electron Microscopy (SEM) for their physicochemical and structural.

Keywords: Biomaterials, Characterisation, Titanium, Bone Scaffold

1. INTRODUCTION

Bone is a complex living tissue with significant metabolic and regenerative activities which are disrupted when the tissue is damaged. Compromised healing may lead to bone non-union, and infection resulting in poor vasculature, decreased cell growth, and scaffolds' inability to integrate with the healthy bone. The use of synthetic bone scaffolds in restoring damaged bone and injuries have been investigated widely in recent years. Diana et al. investigated the mechanical and chemical properties of chitosan/hydroxyapatite scaffolds synthesised via two different methods. It was reported that the commercial hydroxyapatite scaffold had enhanced mechanical properties while in situ hydroxyapatite scaffold exhibited greater morphological properties making it more suitable for tissue engineering applications [1].

Failure to integrate the healthy bone and synthetic scaffolds persist due to the significant challenge arising from the incompatibilities of the scaffold and the actual bone tissue. Natural bone consists of a cancellous and cortical bone with both types exhibiting different morphological, mechanical and chemical properties. Scaffolds for restoring damaged bone should be engineered for enhancing biocompatibility, expressing antibacterial properties to reduce or prevent the proliferation of infectious bacteria, and the correct environment for healthy bone cells to proliferate and integrate. Previous studies focused on mechanical, morphological, and chemical properties separately without considering bacterial growth during the integration phase. Therefore, further studies need to be investigated relating to dual-layered scaffolds, bone integration, and the potential for preventing bacterial proliferation.

This study aims to fabricate antibacterial two-layered synthetic titanium-chitosan bone scaffolds and characterise using a host of structural and biological characterisation techniques. The synthesised scaffolds are analysed using Fourier Transform Infrared Spectroscopy (FTIR), Raman spectroscopy, and Scanning Electron Microscopy to ascertain the structural features that may yield the optimal mechanical and biological response for bone regeneration.

2. MATERIALS AND METHODS

2.1 Synthetic Cortical Biomaterial

Type-1 biomaterials were prepared by mixing different ratios (30%, 40%) of titanium powder with 10% iron-doped brushite mineral. Appropriate quantities of potassium chloride (KCl) powder (0, 20, 40 (v) %) were added as space holders for controlling the overall distribution of interconnected porosity in the cortical structure. The mixtures were pressed into pellets. After pressing, each pellet was cleaned by sonicating the place-holder KCl and

then washed with ethanol before drying at 50ºC in an oven in the air. The pellets were heat-treated at 800ºC for 2 hours in a furnace where flowing argon gas was maintained at the rate of 2 litre min^{-1}. The pellets were cooled down to room temperature after heat-treatment by switching off the furnace power supply. The cooled pellets were analysed for the phases formed and microstructure analysis, as shown below, using the scanning electron microscopic technique.

2.2 Synthetic Cancellous Material

The cancellous synthetic biomaterial was fabricated using chitosan, cerium oxide and brushite.

3wt% chitosan solution was prepared by dissolving high molecular weight chitosan flakes in 2% (v/v) acetic acid solution. The chitosan solution was stirred for 24 hours at room temperature using a magnetic stirrer. For cell and bacterial culture studies, 15 ml of chitosan solution was drawn into cell-culture wells and then frozen for 24 hours at -80˚C. Following freezing, the biomaterial was placed into a freeze-dryer chamber, set at -100˚C and 43 mTorr pressure. The measured pH was 4.95.

Cerium oxide nanoparticles were synthesised by mixing 0.1 M cerium nitrate hexahydrate. The nitrate solution was mixed slowly with 0.3 M NaOH dissolved in deionised water (see equation 1). The mixture was then heated above 50ºC on a hot plate and stirred until the colour of the solution turned light-pink. The pH was maintained at 6.3. The precipitated cerium oxide nanoparticles were centrifuged at 5,000 rpm for separating the solution from the cerium oxide nanoparticles.

$$Ce(NO_3)_3 6H_2O + 3NaOH \rightarrow Ce(OH)_3 + 3NaNO_3 + 6H_20 \qquad \text{(eq. 1)}$$

In this investigation, the brushite mineral was one of the main constituents of the synthetic cancellous bone scaffold. The calcium to phosphate ratio of brushite is Ca P=1:1, which is much lower than hydroxyapatite (HAp), i.e., Ca: P= 3:5. It is reported that the HAp does not resorb readily in the body fluid compared with brushite [2-3]. Without mineral resorption, neo osteogenesis *in situ* does not occur readily, which slows down the formation of new bone structure and, therefore, compromises the healing of damaged bone.

The synthesis of 10wt% iron oxide doped brushite was carried out by dropwise mixing of 0.1 M of calcium nitrate solution with 0.1 M of ammonium phosphate solution, which lasted for 2 hours for a 400 ml volume of solution.

$$Ca(NO_3)_2 \cdot 4H_2O + HPO_4(NH_4)_2 \rightarrow CaHPO_4 \cdot 2H_2O + 2NH_4NO_3 + 2H_2O \qquad \text{(eq.2)}$$

2.3 Fabrication of Scaffold

The fabrication of the Type-2 scaffolds was carried out by mixing cerium oxide, chitosan, and iron-doped brushite mineral in a batch of 10 ml suspension by stirring for 2 hours on a hot plate. During mixing, the temperature was 35ºC, and the measured pH was 4.2.

After mixing, the suspension samples were drawn using a syringe and transferred into the 24 wells for cell and bacterial growth studies. Each solution was kept for 24 hours at -80ºC in a freezer; afterwards, each frozen sample was transferred into a freeze-drier for 24 hours. The process of freeze-drying joined together the synthetic cortical and trabecular parts of biomaterials as one physical structure. The scaffolds were characterised for the structural and microstructural properties for subsequent investigation on biological and physicochemical properties for the infection resistance during osteogenesis and ossification.

3. RESULTS and DISCUSSION

Raman and FTIR spectroscopic methods supplement the synthesised' vibrational structure analysis and help identify the structural changes before and after a chemical reaction, for example. Raman spectroscopy of human bone was investigated for analysing the overall health of the bone by quantifying the mineral phase analysis, establishing the relationship between the phase and compositional relationship and their effect on mechanical properties. Raman spectroscopy has also been used transcutaneously to analyse bone compositions in murine models [4].

This investigation analysed the synthesised Type-1 and Type-2 materials using the FTIR and Raman spectroscopy using a 785 nm excitation source in a Renishaw Invia Raman spectrometer. The laser beam was focussed onto the scaffold surface using a 50x microscope objective, and the scattered light was also collected through this objective for data processing.

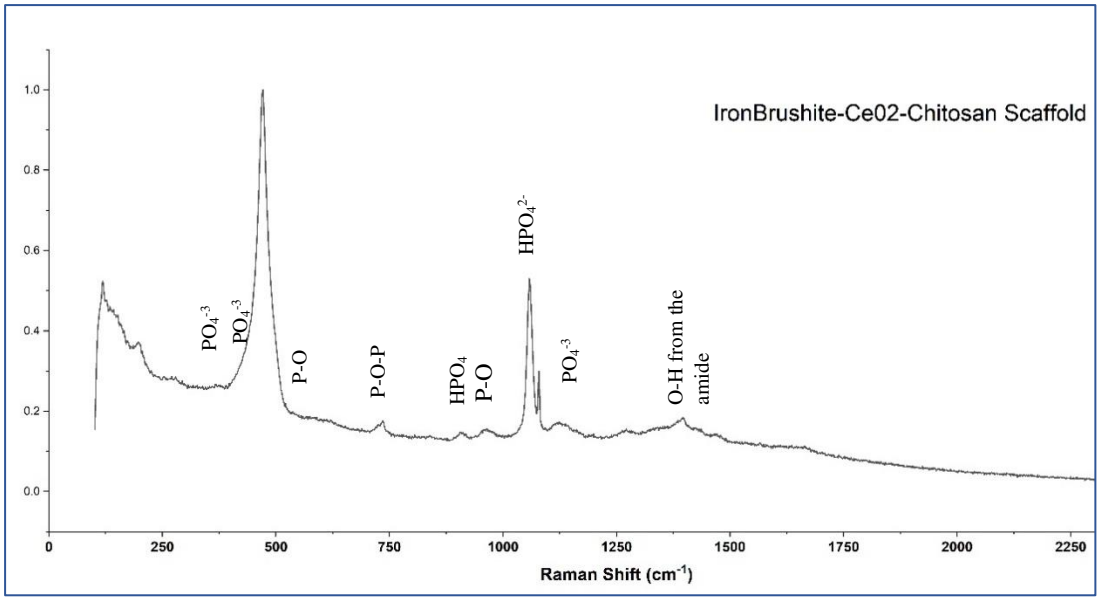

Figure 1. Normalized Raman Spectra of iron-doped brushite- CeO_2-chitosan scaffold

Table 1. Raman Spectra of bone and Type 2 samples material (demonstrated in Figure 1),

Wavenumber (cm^{-1})	Vibration Modes of Type2	Vibration Modes of Bone
436, 590, 988	Symmetric bending of P-O	P-0 [5]
882, 1150	HPO_4^{-2}	Phosphate [5]
385, 420	Lower frequency vibration of PO_4^{-3}	Phosphate [5]
1370	O-H bending	Amide III comes from collagen [5]

The Raman spectra peaks between 280 cm^{-1} and 123 cm^{-1} are associated with Fe-O or/and P-O bending mode. The peaks shown in Figure 1 are from the Type-2 scaffold and confirm the presence of several vibrational modes for the P-O symmetric stretching of the PO_4^{3-} located at approximately 436 cm^{-1}, 590 cm^{-1} and 988 cm^{-1}. The Raman peaks at 882 cm^{-1} and 1150 cm^{-1} correspond to HPO_4^{2-}. The peaks at 385 and 420 cm^{-1} are related lower frequency vibration of PO_4^{-3}. O-H bending Raman spectra peak is located at 1370 cm^{-1}. Also, the CeO_2 peak is present at approximately 460 cm^{-1}.

The FTIR measurements of samples were carried out using the ATR module in the Vertex 70 in the mid-IR range. In Figure 2, the dominant peaks are identified, and the vibrational band assignments are presented in Table 2.

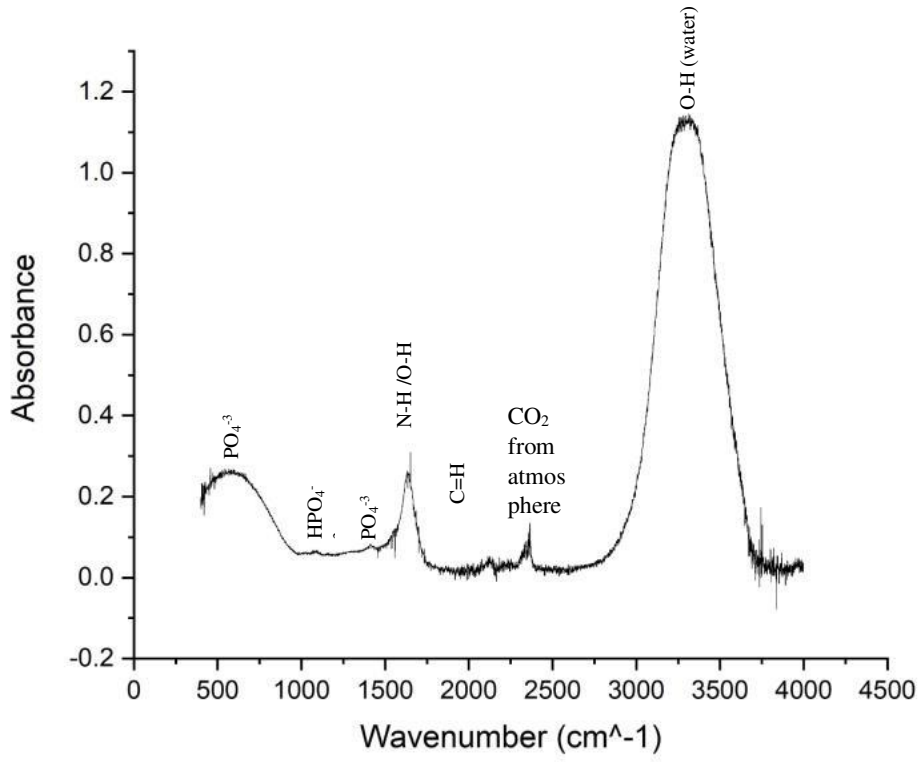

Figure 2. FTIR-ATR spectrum of Type 2 material, the data obtained between 400cm^{-1} and 4000 cm^{-1}.

Table 2. *Band assignments for the FTIR spectra of bone and type 2 material (demonstrated in Figure 2).*

Wavenumber (cm^{-1})	Vibration Modes of Type2	Vibration Modes of Bone
557, 1012	PO_4^{-3} bend	PO_4^{-3} bend (mineral) +Amide (organic) [6]
1117, 1257	HPO_4^{-2}	Amide III (Amide III is not HPO_4^{2-}). Amide peaks are arising from the collagen in bone [6].
1634	C=H	Amide I, Amide peaks are arising from the collagen in bone. Please check. Check collagen FTIR [6].
1541	N-H, O-H	Amide II (collagen in bone) [6]

The peaks at 557 cm^{-1} and 1012 cm^{-1} are assigned to $PO4^{-3}$ stretching mode, whereas the HPO_4^{-2} bending mode peaks are at 1117 cm^{-1} and 1257 cm^{-1}.

From the Raman and FTIR data analysis, it is evident that the molecular structure of chitosan and phosphate mineral has formed a mixed organic-inorganic structure, requiring more detailed structural investigations.

Scanning Electronic Microscopy (SEM, A Hitachi SU8230 1-30 KV Cold field issue pistol) was used for analysing the microstructure of the cortical scaffold surface. The scaffold's Type-1 and Type-2 parts were analysed using the SEM/EDX technique. The identification of the elements present in phases formed in the Type-1 sintered cortical materials was carried out in the SEM using the energy dispersive X-ray analysis. The EDX data was then processed using AZTEC software.

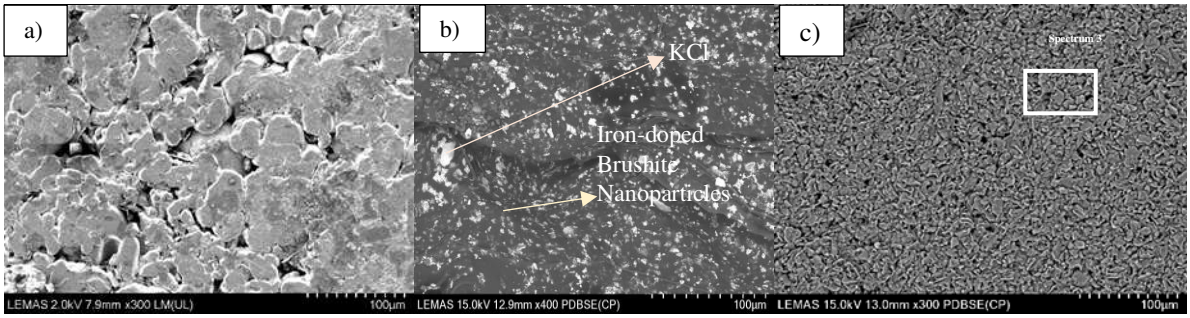

Figure 3. SEM images showing the morphology of a) Type 1 material b) Distribution of KCl in the mineral-Ti powder matrix before sonicated cleaning of pressed pellets of Type-1 scaffold material. The bright phases are KCl and iron-oxide rich regions in the brushite matrix. c) low magnification secondary electron image of Type 2 scaffold material. The rectangle shown in Figure 3c was also analysed using EDX in Figure 5.

In Figure 3a, the secondary electron image shows the morphology of the Ti-alloy surface with intergranular porosity left after sintering at 850 ºC. Figure 3b the fine dispersion of KCl and iron oxide-rich brushite in the backscattered image. Figure 3c shows the interspersed image of brushite mineral, CeO_2, and chitosan in the Type-II material. A more detailed microstructural analysis is shown below.

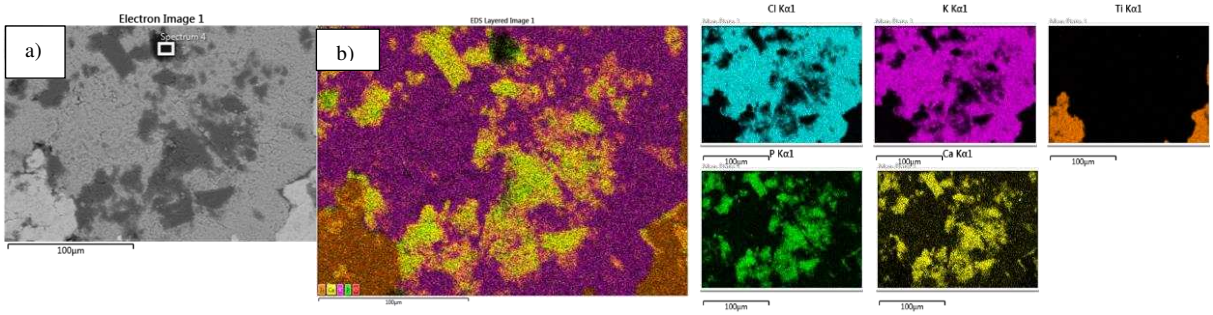

Figure 4. SEM EDX image of 40% Type-I scaffold after sintering: a) the backscattered electron image area analysed for a collection of EDX elemental maps for the phases present; b) EDX area analysed for elemental analysis in phases present (Brushite, Potassium Chloride (KCl) and Titanium alloy:).

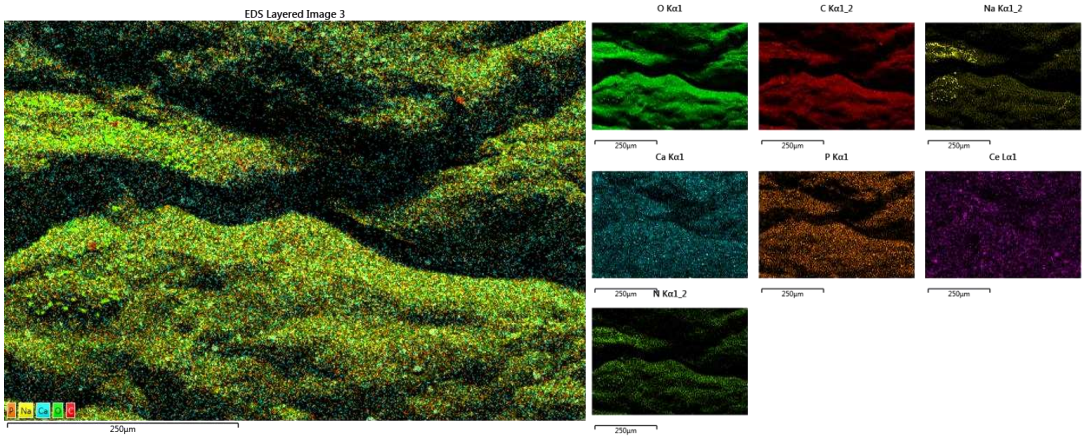

Figure 5. EDX elemental analysis of Type-2 material spectrum 3 (demonstrated in Figure 3c).

The elemental analysis for the phases present confirms the presence of the following elements in weight percent (wt.%): Ca (93%), O (2%), Cl (1.5%), P (2.8%), K (1.5%) and Ti (0.2%).

4. CONCLUSIONS

Morphological and chemical analyses of the Type-1 and Type-2 biomaterials were carried out using the SEM-EDX, FTIR and Raman spectroscopic analysis. The fabricated Type-1 materials show the presence of porosity, which was confirmed by the SEM-EDX analysis. The Type-2 materials were investigated via solution mixing, cryogenic freezing at -80ºC and freeze-drying at -100ºC. The resulting chemical characterisation using FTIR and

Raman of the materials shows the evidence for organic-inorganic phase mixture, which requires a more detailed analysis. The SEM-EDX analysis of the mixture also confirms that the mixing of the inorganic and organic constituents may be taking place on a sub-micrometre scale.

Acknowledgements

This PhD study is supported by the Republic of Turkey, Ministry of Turkish National Education and The School of Chemical Processing Engineering, University of Leeds. This work is also partly supported by the EU PROJECTs, ISMarD and SBR.

REFERENCES

1.) Escobar-Sierra, D. M., Martins, J., & Ossa-Orozco, C. P. Chitosan/hydroxyapatite scaffolds for tissue engineering manufacturing method effect comparison Comparación del efecto del método de fabricación en plataformas de quitosano.

2.) Habraken, W., Habibovic, P., Epple, M., & Bohner, M. (2016). Calcium phosphates in biomedical applications: materials for the future? Materials Today, 19(2), 69-87.

3.) Samavedi, S., Whittington, A. R., & Goldstein, A. S. (2013). Calcium phosphate ceramics in bone tissue engineering: a review of properties and their influence on cell behavior. Acta biomaterialia, 9(9), 8037-8045.

4.) Turunen, M. (2013). Spectroscopic Characterisation of Bone Composition: Alterations during Bone Formation, Maturation and Aging (Doctoral dissertation, Itä-Suomen yliopisto).

5.) Morris, M. D., & Mandair, G. S. (2011). Raman assessment of bone quality. Clinical Orthopaedics and Related Research®, 469(8), 2160-2169.

6.) Figueiredo, M. M., Gamelas, J. A. F., & Martins, A. G. (2012). Characterisation of bone and bone-based graft materials using FTIR spectroscopy. Infrared spectroscopy-life and biomedical sciences, 315-338.